

3D-QSAR Modeling and Molecular Docking Studies on a series of 1,2,4 triazole containing diarylpyrazolyl carboxamide as CB1 cannabinoid receptor ligand

Abstract: 3D-QSAR (comparative molecular field analysis (CoMFA) and comparative molecular similarity indices analysis (CoMSIA)) and Surflex-docking studies were performed on a series of 1,2,4 triazole containing diarylpyrazolyl carboxamide as CB1 cannabinoid receptor ligand as anti-obesity agents. The CoMFA and CoMSIA models using 20 compounds in the training set gave Q^2 values of 0.9 and 0.93, and r^2 values of 0.98 and 0.97, respectively. The adapted alignment method with the suitable parameters resulted in reliable models. The contour maps produced by the CoMFA and CoMSIA models were employed to rationalize the key structural requirements responsible for the activity. Surflex-docking studies revealed that the R3 site, the amine on 1,2,4 triazol group, and the carbonyl were significant for binding to the receptor, some essential features were also identified. Based on the 3D-QSAR and docking results, a set of new molecules with high predicted activities were designed. The total scoring of inactive, active and proposed compounds were compared to each other to determine the best energy affinity.

Keywords: 3D-QSAR; CoMFA; CoMSIA; Surflex-docking; Anti-obesity; 1,2,4 triazole.

1. Introduction

Triazoles are the class of heterocyclic compounds, which are under study since many years [1]. Azoles moieties are an important and frequent insecticidal, agrochemical structure feature of many biological active compounds such as cytochrome p450 enzyme inhibitors [2], peptide analog inhibitors [3], and 3, 5 disubstituted 1,2,4 triazole derivatives [4-6] were also reported to show fungicidal, herbicidal, anti-inflammatory, and anticonvulsant [7-12]. Chemistry of 1,2,4 triazole and their derivatives have received considerable attention owing to their synthetic and biological importance. 1,2,4 triazole moiety have incorporated into variety of therapeutically interesting drug candidates including antiviral, antimigraine, antifungal, antianxiety, insecticidal, antimicrobial [13-15], and some showed tyrosinase inhibitors [16], cannabinoid receptor antagonist activities [17].

In the present study 1,2,4 triazole ring is attached with diarylpyrazolyl carboxamide shows cannabinoid receptor binding affinity or antiobesity activity through the down-regulation of the endocannabinoid system by the specific blockage of CB1 receptors could induce body weight reduction [18].

Recently the advancement of computational chemistry led to new challenges of drug discovery. Structure-activity relationship (3D-QSAR) methods along with docking approaches were used to explore the structure-activity relationship (SAR) of compounds. Comparative molecular field analysis

(CoMFA) [19] and comparative molecular similarity indices analysis (CoMSIA) [20], were performed to predict the activities of these molecules and offered the regions where interactive fields (steric, electrostatic, hydrophobic, hydrogen bond donor and hydrogen bond acceptor fields) may increase or decrease the activity. The core idea of the present study is searching for novel 1,2,4 triazole containing diarylpyrazolyl carboxamide as CB1 Cannabinoid receptor- ligand that would show useful antiobesity activity, relying on those developed models. Surflex-Docking was applied to study the interactions between the inactive, active and the proposed compounds with CB1 cannabinoid receptor (PDB entry code: **2MZ2**). To compare the energy affinity of the proposed ligands and the active compound of the series, we calculate total scoring of the stable conformation. Furthermore, we design a new 1,2,4 triazole containing diarylpyrazolyl carboxamide derivatives by utilizing the structure information obtained from the CoMFA and CoMSIA models, which exhibit excellent predictive potencies. Moreover, based on the admirable performance of docking studies, the predicted activities of these newly designed molecules show an excellent energy affinity compared to the compounds in [table 1](#).

2. Materials and methods

A database of 26 compounds obtained from literature [21] consisted of 1,2,4 triazole containing diarylpyrazolyl carboxamide as CB1 cannabinoid receptor-ligand as anti-obesity agents, the data set was split into two sets, a 20 compounds were selected as training set and 6 compounds were selected as test set, based on a random selection to evaluate the ability of the model obtained. The structures and biological activities of all the training and test set compounds are given in [table 1](#). This data set used to construct 3D-QSAR (CoMFA and CoMSIA) model and to analyze their physicochemical properties. The IC_{50} values were converted to pIC_{50} , used as dependent variable in the QSAR study, according to the formula described in equation 1.

$$pIC_{50} = -\log IC_{50} \quad (1)$$

Three-dimensional structure building and all modeling were performed using the Sybyl 2.0 program package.

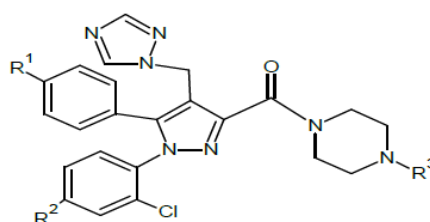


Figure 1: Chemical structure of the studied compounds

Table 1: Chemical structures and anti-obesity activities of 1,2,4 triazole containing diarylpyrazolyl carboxamide derivatives

No	Structure			pIC ₅₀
	R ₁	R ₂	R ₃	
1 **	H	H	H	8.34
2	Cl	Cl	Me	5.84
3	Cl	Cl	Phenyl	8.05
4 *	Cl	Cl	3-Chloro phenyl	8.05
5	Cl	Cl	2,3-dichloro phenyl	8.26
6	Cl	Cl	2,3-dimethyl phenyl	7.94
7 *	Cl	Cl	2-pyrimidyl	7.25
8	Cl	H	Methyl	6.02
9	Cl	H	Ethyl	5.98
10	Cl	H	Phenyl	7.94
11	Cl	H	3-Chlorophenyl	8.39
12	Cl	H	2-3-Dimethylphenyl	8.22
13	Br	Cl	Methyl	5.87
14	Br	Cl	Ethyl	6.55
15	Br	Cl	Phenyl	7.90
16	Br	Cl	3-chlorophenyl	8.14
17	Br	Cl	2,3-Dichlorophenyl	8.24
18	Br	Cl	2,3-Dimethylphenyl	8.42
19 *	Br	Cl	2-Pyrimidyl	7.56
20	Br	H	Methyl	6.05
21	Br	H	Ethyl	6.52
22	Br	H	Phenyl	8.10
23	Br	H	3-Chlorophenyl	8.64
24	Br	H	2,3-Dichlorophenyl	8.65
25 *	Br	H	2,3-Dimethylphenyl	8.68
26 *	Br	H	2-Pyrimidyl	7.65

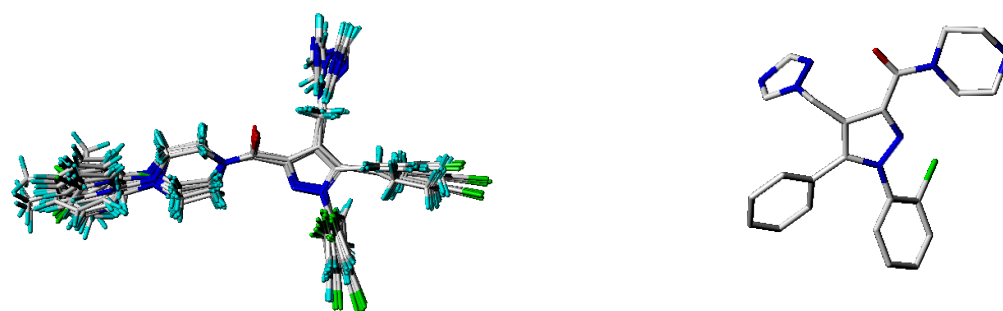
* Test set molecules

** Outlier compound

2.1. Minimization and alignment

Molecular structures were sketched with sketch module in SYBYL and minimized using Tripos force field [22] with the Gasteiger–Huckel charges [23] and conjugated gradient method, and gradient convergence criteria of 0.01 kcal/mol. Simulated annealing on the energy minimized structures was performed with 20 cycles. All 26 compounds were minimized to get the low energy conformation of each compound. The fragment 1(the core) is the common structure to all 26 compounds that were considered in this study, and The most active compound (compound **25**) was used as an alignment template . all molecules were aligned with respect to this fragment, using the simple alignment method in Sybyl [24]. The superimposed structures of aligned data set are shown in [figure 2](#).

82



83

84

Aligned compounds

85

Figure 2: 3D-QSAR structure superposition and alignment of training set using molecule 25 as a template

86

87 2.2. Outliers

88 Outliers in the QSAR studies are usually the result of an improper calculation of some molecular
89 descriptors and/or experimental error in determining the property to modelled. They influence greatly
90 any least square model, and therefore the conclusions about the biological activity of a potential
91 component based on such a model are misleading.

92 2.3. 3D-QSAR Studies

93 To understand and explore the contributions of electrostatic, steric and hydrophobic fields of the data
94 set and to build predictive 3D-QSAR models, CoMFA and CoMSIA studies were performed based on
95 the molecular alignment strategy. The 3D-QSAR studies were performed as previously described in the
96 literature.

97 2.4. CoMFA and CoMSIA

98 Based on the molecular alignment, CoMFA and CoMSIA studies were performed to analyze the
99 specific contributions of steric, electrostatic, and hydrophobic effects. CoMFA calculates steric and
100 electrostatic properties according to Lennard Jones and Coulomb potentials, respectively, whereas
101 CoMSIA calculates the similarity indices in the space surrounding each of the molecules in the dataset.
102 CoMFA steric and electrostatic interaction fields were calculated at each lattice intersection point of a
103 regularly spaced grid of 2.0 Å. The default value of 30 kcal/mol was set as a maximum steric and
104 electrostatic energy cutoff [25]. With standard options for scaling of variables, the regression analysis
105 was carried out using the full cross-validated partial least squares (PLS) method (leave-one-out) [26].
106 The minimum sigma (column filtering) was set to 2.0 kcal/mol to improve the signal-to-noise ratio by
107 omitting those lattice points whose energy variation was below this threshold. The final non-cross-
108 validated model was developed using optimal number of components that had both the highest Q^2
109 value and the smallest value of standard error predictions. The predictive r^2 was used to evaluate the
110 predictive power of the CoMFA model, and was based only on test set. Several CoMFA models were

built by considering permutations of molecules between training and test sets. The best model amongst them was chosen on the basis of high Q^2 , r^2 values and small Standard Error of Estimate (SEE) value. In CoMSIA, a distance-dependent Gaussian-type physicochemical property has been adopted to avoid singularities at the atomic positions and dramatic changes of potential energy for grids being in the proximity of the surface. With the standard parameters and no arbitrary cutoff limits, five fields associated to five physicochemical properties, namely steric (S), electrostatic (E), and hydrophobic effects (H) and hydrogen bond donor (D) and acceptor (A) were calculated. The steric contribution was reflected by the third power of the atomic radii of the atoms. The electrostatic descriptors are derived from atomic partial charges, the hydrophobic fields are derived from atom-based parameters developed by Viswanadhan and the hydrogen bond donor and acceptor indices are obtained by a rule-based method derived from experimental values [27].

2.5. PLS analysis

Partial least squares statistical method used in deriving the 3D-QSAR models is an extension of multiple regression analysis in which the original variables are replaced by a small set of their linear combinations. PLS method with leave-one-out (LOO) cross-validation was used in this study to determine the optimal numbers of components using cross-validated coefficient Q^2 . The external validation of various models was performed using a test set of five molecules. The final analysis (non-cross-validated analysis) was carried out using the optimum number of components obtained from the cross-validation analysis to get correlation coefficient (R^2). The Q^2 value determines the internal predictive ability of the model while R^2 value evaluates the internal consistency of the model. Thus, the best QSAR model was chosen on the basis of a combination of Q^2 and R^2 .

2.6. Y-Randomization Test

The obtained models were further validated by the Y-Randomization method. The Y vector (pIC_{50}) is randomly shuffled many times and after every iteration, a new QSAR model is developed. The new QSAR models are expected to have lower Q^2 and r^2 values than those the original models. This technique is carried out to eliminate the possibility of the chance correlation. If higher values of the Q^2 and r^2 are obtained, it means that an acceptable 3D-QSAR can't be generated for this data set because of structural redundancy and chance correlation.

139

140

2.7. Molecular Docking

The Surflex-Dock was applied to study molecular docking by using an empirical scoring function and a patented search engine to dock ligands into a protein's binding site [28]. The crystal structure of CB1 cannabinoid receptor was retrieved from the RCSB Protein Data Bank (PDB entry code: **2MZZ**). The

ligands were docked into corresponding protein's binding site by an empirical scoring function and a patented search engine in Surflex-Dock [28]. All water molecules in **2MZ2** have been deleted and the polar hydrogen atoms were added. Protomol, a representation of a ligand making every potential interaction with the binding site, was applied to guide molecular docking.

Protomols could be established by three manners: (1) Automatic: Surflex-Dock finds the largest cavity in the receptor protein; (2) Ligand: a ligand in the same coordinate space as the receptor; (3) Residues: specified residues in the receptor [29,30].

In this paper, the automatic docking was applied. The **2MZ2** structure was utilized in subsequent docking experiments without energy minimization. Other parameters were established by default in the software. Surflex-Dock scores (total scores) were expressed in $-\log_{10}(K_d)$ units to represent binding affinities. Then, the MOLCAD (Molecular Computer Aided Design) program was employed to visualize the binding mode between the protein and ligand. MOLCAD calculates and exhibits the surfaces of channels and cavities, as well as the separating surface between protein subunits [31–33]. MOLCAD program provides several types to create a molecular surface [28]. The fast Connolly method using a marching cube algorithm to engender the surface was applied in this work, thus the MOLCAD Robbin and Multi-Channel surfaces program exhibited with copious potentials were established. Moreover, Surflex-Dock total scores, which were expressed in $-\log_{10}(K_d)$ units to represent binding affinities, were applied to estimate the ligand-receptor interactions of newly designed molecules. Each single optimized conformation of each molecule in the data set was energetically minimized employing the Tripos force field and the Powell conjugate gradient algorithm with a convergence criterion of 0.05 kcal/mol Å° and Gasteiger-Huckel charges.

3. Results and Discussion

The predicted and experimental activity values and their residual values for both the training and test sets from CoMFA and CoMSIA models are given in [table 2](#).

3.1. CoMFA results

PLS summary [table 2](#) shows that CoMFA model has high R^2 (0.98), F (167.22), and a small S_{cv} (0.137), as well as a great cross-validated correlation coefficient Q^2 (0.90) with four as optimum number of components. The external predictive capability of a QSAR model is generally cross checked and validated using test sets. The five test sets which were selected randomly were optimized and aligned as same as training sets. Moreover the predicted correlation coefficient r^2_{pred} (0.94) represents that prediction ability of CoMFA model is excellent.

The contributions of steric to electrostatic fields were found to be 90:09, which indicate that the interaction of steric field is extremely important to consider the model have a good quality and

predictive capability, and this is in agreement with the hydrophobic character of the cannabinoid ligands.

3.2. CoMSIA results

Based on CoMSIA descriptors available on SYBYL a 3D-QSAR model was proposed to explain and predict quantitatively the Hydrophobic, Electrostatic, steric, donor and acceptor fields effects of substituents on CB1 cannabinoid receptor ligand as anti-obesity activity of twenty six 1,2,4 triazole containing diarylpyrazolyl carboxamide compounds.

Different combinations of the five fields were generated. The best CoMISA proposed model contains four fields (Steric, Electrostatic, Hydrophobic, and Acceptor), the cross-validated correlation coefficient Q^2 value of the training set and non-cross-validated correlation coefficient r^2 are 0.93 and 0.97, respectively. The optimal number of principal components using to generate the CoMSIA model is 3, which is reasonable considering the number of molecules used to build the model. The standard error was 0.175. Finally, the prediction ability of the proposed model was confirmed using the external validation, the r_{ext}^2 value obtained is 0.97. Those statistics results indicated the very good stability and the powerful predictive ability of CoMSIA model.

Table 2 : PLS Statistics of CoMFA and CoMSIA models

Model	Q^2	r^2	S_{cv}	F-t	N	R_{ext}^2	Fractions				
							Ster	Elec	Acc	Don	Hyd
CoMFA	0.90	0.98	0.137	167.22	4	0.94	0.902	0.098	-	-	-
CoMSIA	0.93	0.97	0.175	149.73	3	0.97	0.367	0.153	0.159	0.00	0.321

Q^2 : Cross-validated correlation coefficient.

N : Optimum number of components.

r^2 : Non-cross-validated correlation coefficient.

S_{cv} : Standard error of the estimate.

F : F -test value

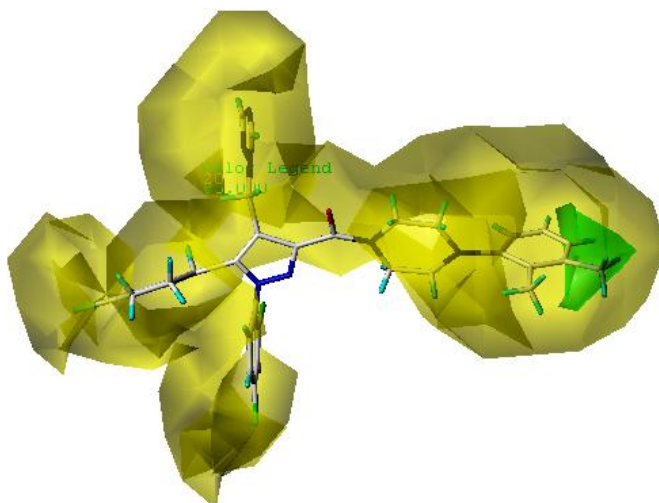
r_{ext}^2 : External validation correlation coefficient.

3.3. Graphical Interpretation of CoMFA and CoMSIA

CoMFA and CoMSIA contour maps were generated to rationalize the regions in 3D space around the molecules where changes in each field were predicted to increase or decrease the activity. The CoMFA steric and electrostatic contour maps that are shown in figure 3. Steric, hydrophobic and hydrogen bond acceptor contour maps of CoMSIA are shown in figure 4. Using compound **18** as reference structure. All the contours represented the default 80% and 20% level contributions for favored and disfavored regions respectively.

210 **CoMFA Contour Maps**

211 CoMFA electrostatic interactions are represented by red and blue colored contours while steric
212 interactions are represented by green and yellow colored contours. The bulky substituents are favored
213 in the green regions and at yellow regions, they are unfavored. The blue regions indicate that positive
214 charges are favored, and red regions increase activity only with negative charges.



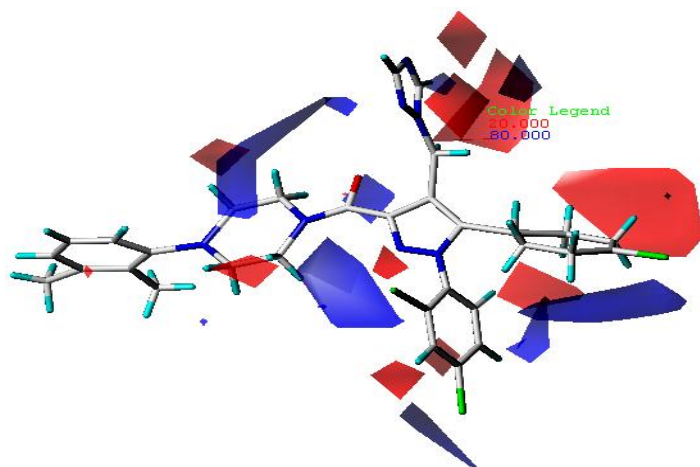
215

216 Figure 3a: Std* coeff. contour maps of CoMFA analysis with 2 Å grid spacing in combination with compound **18**. Steric
217 fields: green contours (80% contribution) indicate regions where bulky groups increase activity, while yellow contours
218 (20% contribution) indicate regions where bulky groups decrease activity

219

220 As figure 3a shows, the yellow contour near R1, R2 position indicates that addition of bulky groups
221 would decrease the potency. Whereas the green region around the R3 position indicates, that bulky
222 group is favored and they might increase the activity. The yellow and green contours can explain very
223 well The discrepancies of Comparing compound **13** (R3=Methyl) with $pIC_{50}=5.87$ and **25** (R3= 2,3-
224 Dimethylphenyl) with $pIC_{50}=8.68$.

225



226

227 Figure 3b: Std* coeff. Contour maps of CoMFA analysis with 2 Å grid spacing in combination with compound **18**.
228 Electrostatic fields: blue contours (80% contribution) indicate regions where groups with negative charges increase activity,
229 while red contours (20% contribution) indicate regions where groups with positive charges increase activity

230

The red contour near the R2 position indicates that groups with positive charges may increase the activity. This explain why compound **2** (**R2**=Cl) with electron-donating substituent at this position is an inactive derivative. A blue contour near the R1 position demonstrated that electron-donating groups would benefit the activity, this explain why compounds **23** (pIC_{50} =8.64), **24** (pIC_{50} =8.65) and **25** (pIC_{50} =8.68) have an electron-donating substituent at R1 (**R1**=Br) showed significantly increased activities.

CoMSIA Contour Map

The CoMSIA steric and electrostatic field contour maps were almost similar to the corresponding CoMFA contour maps.

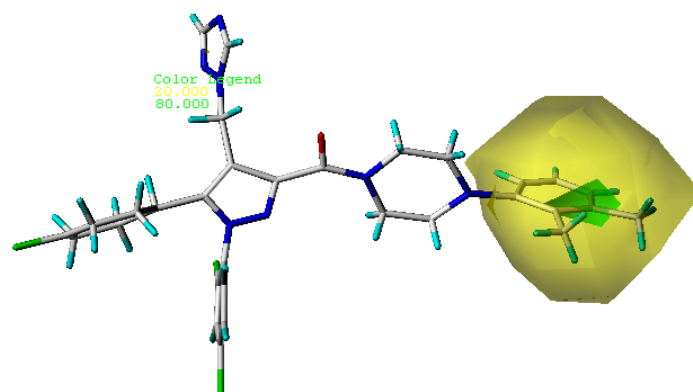


Figure 4a: Std* coeff. contour maps of CoMSIA analysis with 2 Å grid spacing in combination with compound **18**. Steric fields: green contours (80% contribution) indicate regions where bulky groups increase activity, while yellow contours (20% contribution) indicate regions where bulky groups decrease activity

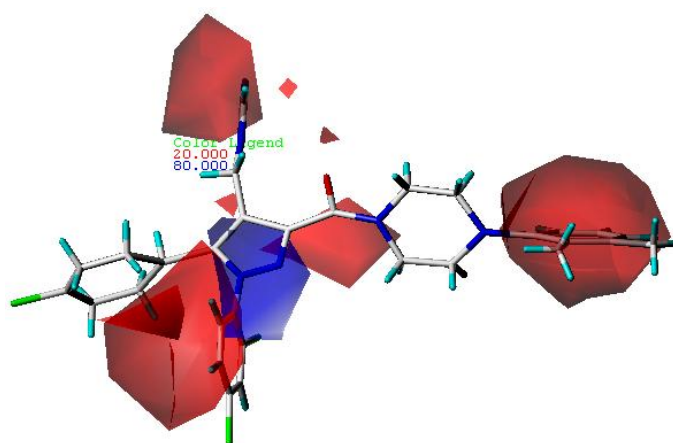


Figure 4b: Std* coeff. contour maps of CoMSIA analysis with 2 Å grid spacing in combination with compound **18**. Electrostatic fields: blue contours (80% contribution) indicate regions where electron-donating groups increase activity, while red contours (20% contribution) indicate regions where electron-withdrawing groups increase activity

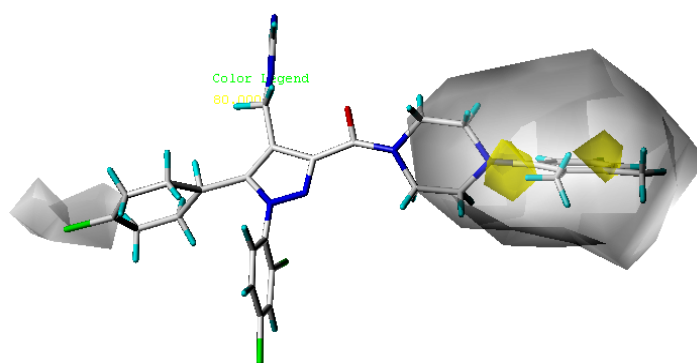


Figure 4c: Std* coeff. contour maps of CoMSIA analysis with 2 Å grid spacing in combination with compound **18**. Hydrophobic fields: yellow contours (80% contribution) indicate regions where hydrophobic properties were favored, while white contours (20% contribution) indicate regions hydrophilic properties were favored

The two yellow contours around R3 (2,3-Dimethylphenyl) indicate that replacing this position with hydrophilic may decrease the activity. The huge white contour around the piperazine cycle and R1 position indicate that hydrophilic groups are favored.

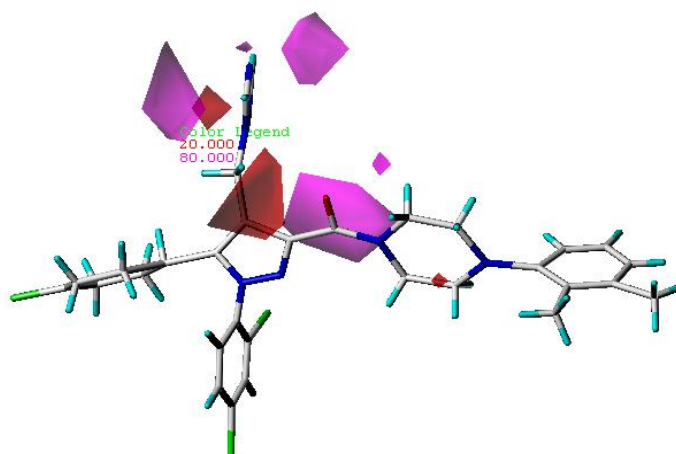


Figure 4d: Std* coeff. contour maps of CoMSIA analysis with 2 Å grid spacing in combination with compound **18**. H-bond acceptor fields: The purple (80% contribution) and red (20% contribution) contours favorable and unfavorable positions for hydrogen bond acceptors respectively

The purple contour around the carbonyl group revealed a hydrogen bond acceptor substituent at this position would increase the activity. The red contour near N position revealed the importance of the hydrogen bond donor -NH group.

Table 3: Experimental and calculated anti-obesity activity (pIC_{50}) with residuals results of compounds in training set and test set for CoMFA and CoMSIA models

Compound No.	Actual pIC_{50}	CoMFA		CoMSIA	
		Predicted pIC_{50}	Residuals	Predicted pIC_{50}	Residuals
2	5.84	5.815	0.025	5.495	0.345
3	8.05	8.013	0.037	8.026	0.024
4*	8.05	7.720	0.330	7.971	0.079
5	8.26	8.353	-0.093	8.164	0.096
6	7.94	8.078	-0.138	7.887	0.053
7*	7.25	7.432	-0.182	7.068	0.182
8	6.02	6.033	-0.013	6.151	-0.131

9	5.98	6.073	-0.093	6.039	-0.059
10	7.94	8.010	-0.070	8.109	-0.169
11	8.39	8.334	0.056	8.196	0.194
12	8.22	8.075	0.145	8.178	0.042
13	5.87	5.740	0.130	5.765	0.105
14	6.55	6.521	0.029	6.802	-0.252
15	7.90	8.018	-0.118	7.949	-0.049
16	8.14	8.143	-0.003	7.981	0.159
17	8.24	8.370	-0.130	8.248	-0.008
18	8.42	8.468	-0.048	8.556	-0.136
19*	7.56	7.982	-0.422	7.815	-0.255
20	6.05	5.953	0.097	6.151	-0.101
21	6.52	6.695	-0.172	7.092	-0.572
22	8.10	8.139	-0.039	8.344	-0.233
23	8.64	8.568	0.072	8.359	0.281
24	8.65	8.701	-0.051	8.356	0.294
25*	8.68	8.114	0.566	8.370	0.310

3.4. Y-Randomization

Table 4: Q^2 and r^2 values after several Y-randomization tests

Iteration	CoMFA		CoMSIA	
	Q^2	r^2	Q^2	r^2
1	0.22	0.92	0.06	0.73
2	0.15	0.60	0.37	0.42
3	0.11	0.80	0.18	0.76
4	-0.60	0.52	-0.15	0.62
5	-0.34	0.84	-0.45	0.72

The Y-Randomization method was carried out to validate the CoMFA and CoMSIA models. Several random shuffles of the dependent variable were performed then after every shuffle, a 3D-QSAR was developed and the obtained results are shown in table 4. The low Q^2 and r^2 values obtained after every shuffle confirmed that the excellent result in our original CoMFA and CoMSIA models are not due to a chance correlation of the training set.

3.5. Design for New molecules with anti-obesity activity

Five new molecules have been designed to enhance the activity, based on the proposed CoMFA and CoMSIA 3D-QSAR models. These compounds were aligned to the database using compound **18** as a template.

The newly predicted structure A showed higher activity ($pIC_{50} = 9.28$ and 8.37 for CoMFA and CoMSIA models respectively) than compound **25** (the most active compound of the series).

Table 5: Chemical structure of newly designed molecules and their predicted pIC_{50} based on CoMFA and CoMSIA 3D-QSAR models

No	Structure			Predicted pIC_{50}	
	R ₁	R ₂	R ₃	CoMFA	CoMSIA
A	I	H	3,5difluoro-4dichloromethylphenyl	9.28	8.37
B	I	H	3,5difluoro-4difluoromethylphenyl	8.98	7.26

C	I	H	4trifluoromethylphenyl	8.85	7.27
D	I	H	2,4,6tribromophenyl	8.69	7.58
E	I	H	5bromo-6chlorophenyl	8.66	8.52

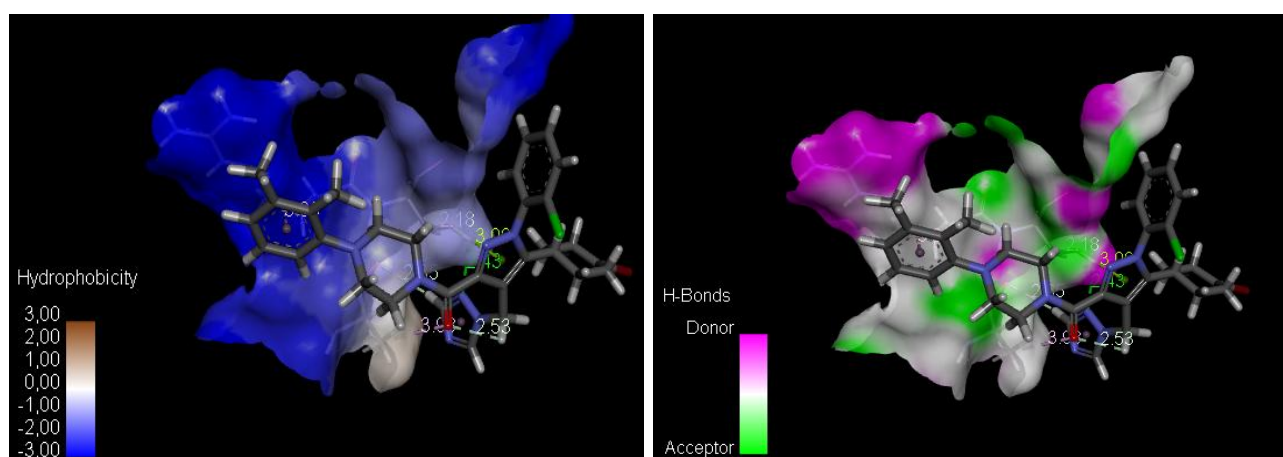
286

287 4. Docking Analysis

288 Surflex-Dock was applied to investigate the binding mode between 1,2,4 triazole containing
 289 diarylpyrazolyl carboxamide (inactive, active and proposed molecules) and **2MZ2** receptor. In this
 290 paper, Surflex-Dock could also serve to inspect the stability of 3D-QSAR models previous established.
 291 To visualize secondary structure elements, the MOLCAD Robbin surfaces and Discovery studio
 292 visualizer programs were applied, to develop electrostatic potential (EP), H-bond and Hydrophobicity
 293 maps, and explore the interaction between the ligand and the receptor. The proposed active molecule
 294 (A) was selected for visualization purposes.

295 The blue color in figure 5 shows hydrophilic character of the ligand, the pink color around R3 group
 296 indicate that H-bond donor groups are favored. In figure 6, the hydrogen bonding (dashed lines)
 297 interactions between the compound A (with highest activity) and the key residues (LYS3, ASP4,
 298 LEU5, and ARG6) of CB1 cannabinoid receptor (PDB code **2MZ2**) are labeled. A total of four
 299 hydrogen bonds were formed: The Fluor at R3 position acted as the hydrogen bond acceptor and
 300 formed two H-bonds with the amino group of the ARG6 residue, the carbonyl group on the ligand also
 301 acted as the hydrogen bond acceptor and formed H-bond with the amino group of LEU5 residue, the
 302 amine on the 1,2,4 triazole groupment acted as H-bond acceptor, and formed H-bond with amino group
 303 of LYS3. These results are satisfactorily matched the observation taken from the CoMSIA contour
 304 maps.

305 In figure 8 , The R3 site was found in a yellow area, which suggested that electron-withdrawing
 306 properties would be favored; The observations obtained from this electrostatic potential surface
 307 satisfactorily matched the corresponding CoMFA and CoMSIA electrostatic contour maps.



308 Figure 5: The interaction H-bond and Hydrophobicity between the active molecule and **2MZ2** receptor, visualized with
 309 Discovery studio visualizer program

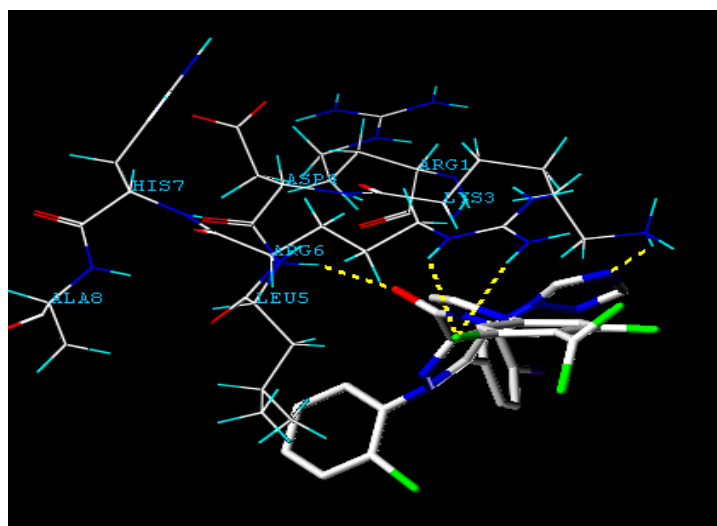


Figure 6: The binding mode between compound **A** and the allosteric site of CB1 cannabinoid receptor (PDB code **2MZ2**)
Key residues and hydrogen bonds are labeled.

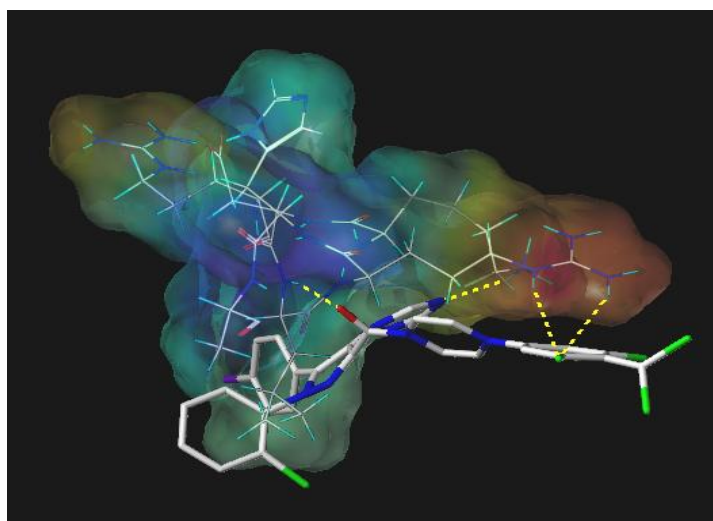


Figure 7: The MOLCAD electrostatic potential surface of the allosteric site within the compound **A**. The color ramp for EP ranges from red (most positive) to purple (most negative).

The surflex-dock total score gives us twenty poses for each molecule, and the stable pose of the inactive structure is the one with a scoring of 1.8, while the active molecule (compound **25**) gives us a scoring with 2.5. The proposed structure (**A**) gives us a stable position with a scoring of 3.25, which indicate that the proposed compound present an excellent activity compared to those listed in [table 1](#).

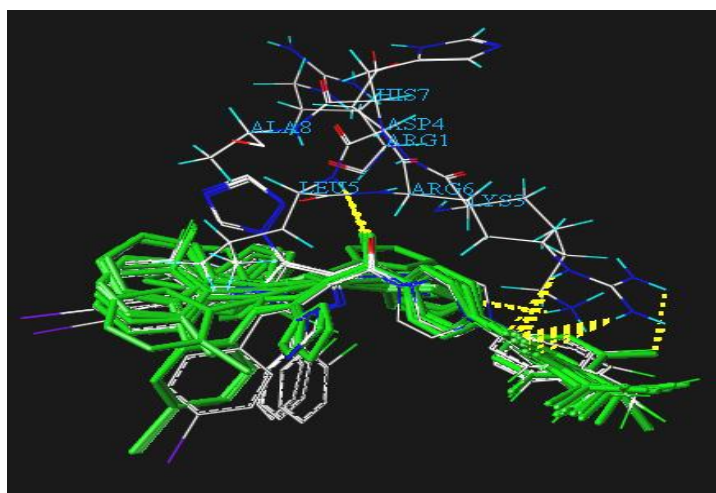


Figure 8: Overlap of the top-ranked docked poses of compounds **A** in the active site of CB1 cannabinoid receptor (PDB code **2MZ2**)

5. Conclusion

3D-QSAR and surflex-docking methods were used to explore the structure-activity relationship of series of 1,2,4 triazole as CB1 cannabinoid receptor (anti-obesity). The excellent predictive ability of CoMFA and CoMSIA observed for the test set of compounds indicated that these models could successfully used to predict the IC₅₀ values. Furthermore, the CoMFA and CoMSIA contour maps results offered enough information to understand the structure-activity relationship and identified structural features influencing the activity. A number of novel derivatives were designed by utilizing the structure-activity relationship taken from present study, based on the excellent performance of the external validation, and total scoring, these newly designed molecules can be trustworthy.

References

- [1] Tirlapur K.V., Tadmalle T. Synthesis and Insecticidal activity of 1,2,4 – Triazolothiazolidin-4-one derivatives, Pelagia research library -231hgdsa z Der Pharmacia sinica2011; 2(1):135-141.
- [2] Vanden Bossche H.J. Steroid Biochem Molec.Biol.1992; 42: 45.
- [3] Meek T.D. J Enzyme inhib.1992; 6: 65.
- [4] Talawar M.B., Laddi U.V., Somannavar Y.S., Benner R.S., Bennur S.C., Indian J Heterocycl.Chem1995;4:297.
- [5] Zhang Z.Y., Yan H. Acta Chimicia Sinica. 1987; 45:403.
- [6] Talawar M.B., Bennur S.C., Kankanwadi S.K., Patil P.A. Indian J.Pharm.Sci 1995; 57:194.
- [7] Ramos M.G.,Bellus D.Angew Chem.1991;103:1689.
- [8] Oita S., Uchida T. Jpn Kokai Tokkyo Koho ,JP, 10212287.11August 1998:7.
- [9] Takao H. Jpn Kokai Tokkyo Koho ,JP, 62108868,20 May 1987;11.

- [10] Shikawa H., Umeda T., Kido Y., Takai N., Yoshizawa H. Jpn Kokai Tokkyo Koho ,JP, 05194432,3August 1993:13.
- [11] Shaker M.R. Chemistry of mercapto and thione substituted 1,2,4 triazoles and their utility in heterocyclic synthesis :Arkivoc 2006;9:59-112.
- [12] Fotouchi L., Heravi M.M., Hekmatshoar R. Rasmi V. Novel electrosynthesis of a condensed thioheterocyclic system containing 1,2,4 triazole ring:Tetrahedron Letters 2008;49:6628-6630.
- [13] Jubie S., Sikdar P., Antony S., Kalirajan R., Gowramma B., Gomathy S., Elango K. Synthesis and biological evaluation of some Schiff Bases of [4-(amino)-5- phenyl-4H- 1,2,4- triazole-3-thiol];Pak.J.Pharm.Sci.April 2011; 24(2):109-112.
- [14] Matsumoto O.,Uekawa T. Jpn Kokai Tokkyo Koho,JP,2000239262,5Sep.2000:13.
- [15] Nakayama Y., Yano T., Jpn Kokai Tokkyo Koho, JP 03068565, 25 Mar.1991:9.
- [16] Nakamura Y., Komatsu H., Yoshihara H., Jpn Kokai Tokkyo Koho,JP 08059675,5Mar.1996:5.
- [17] Ghani U., Ullah N. New potent inhibitors of tyrosinase: Novel clues to binding of 1,3,4-thiadiazole- 2(3H)-thiones,1,3,4- oxadiazole-2(3H)- thiones,4-amino-1,2,4- triazole- 5(4H)-thiones,and substituted hydrazides to the dicopper active site: Bioorg.&Med.Chem.2010;18:4042-4048.
- [18] Seo H.J.,Kim M.J., Lee S.H., Jung M.E., Kim M.S. Ahn K. Synthesis and structure – activity relationship of 1,2,4-triazole- containing diarylpyrazolyl carboxamide as CB1 cannabinoid receptor-ligand.Bioorg.Med.Chem. 2010(18):1149-1162.
- [19] R.D. Cramer III, D.E. Patterson, J.D. Bunnce. Comparative molecular field analysis (CoMFA): 1. Effect of shape on binding of steroids to carrier proteins. J. Am. Chem. Soc. 1988, 110: 5959-5967.
- [20] G. Klebe, U. Abraham, T. Mietzner. Molecular similarity indices in a comparative analysis (CoMSIA) of drug molecules to correlate and predict their biological activity. J. Med. Chem. 1994, 37: 4130-4146.
- [21] Nidhi Gupta, Kamta Prasad Namdeo and Lokesh Sahu. 2d qsar analysis on 1, 2, 4-triazole-containing diarylpyrazolyl carboxamide as cb1 cannabinoid receptor – ligand. Vol 4, Issue 04, 2015.
- [22] M. Clark, R. D. Cramer, and N. Van Opdenbosch, “Validation of the general purpose tripos 5.2 force field,” J. Comput. Chem., vol. 10, no. 8, pp. 982–1012, Dec. 1989.
- [23] W. P. Purcell and J. A. Singer, “A brief review and table of semiempirical parameters used in the Hueckel molecular orbital method,” J. Chem. Eng. Data, vol. 12, no. 2, pp. 235–246, Apr. 1967
- [24]. M. D. M. AbdulHameed, A. Hamza, J. Liu, and C.-G. Zhan, “Combined 3D-QSAR Modeling and Molecular Docking Study on Indolinone Derivatives as Inhibitors of 3-Phosphoinositide-Dependent Protein Kinase-1,” J. Chem. Inf. Model., vol. 48, no. 9, pp. 1760–1772, Sep. 2008.
- [25].L. Ståhle and S. Wold, “Multivariate data analysis and experimental design in biomedical research.,” Prog. Med. Chem., vol. 25, pp. 291–338, 1988.

- 381 [26]. Bush BL, Nachbar RB Jr (1993) Sample-distance partial least squares: PLS optimized for many
382 variables, with application to CoMFA. *J Comput Aided Mol Des* 7:587–619
- 383 [27]. Viswanadhan VN, Ghose AK, Revankar GR, Robins RK (1989) Atomic physicochemical
384 parameters for three-dimensional structure directed quantitative structure-activity relationships. 4.
385 Additional parameters for hydrophobic and dispersive interactions and their application for an
386 automated superposition of certain naturally occurring nucleoside antibiotics. *J Chem Inf Comput Sci*
387 29:163–172
- 388 [28]. *Sybyl 8.1*; Tripos Inc.: St. Louis, MO, USA, 2008; Available online: <http://www.tripos.com>
389 (accessed on 26 January 2011).
- 390
- 391 [29]. Jain, A.N. Surflex: Fully automatic flexible molecular docking using a molecular Similarity-
392 Based search engine. *J. Med. Chem.* 2003, 46, 499–511.
- 393
- 394 [30]. Sun, J.Y.; Cai, S.X.; Mei, H.; Li, J.; Yan, N.; Wang, Y.Q. Docking and 3D-QSAR study of
395 thiourea analogs as potent inhibitors of influenza virus neuraminidase. *J. Mol. Model.* 2010. 16,1809–
396 1818.
- 397 [31]. Ai, Y.; Wang S.T.; Sun, P.H.; Song F.J. Molecular Modeling Studies of 4,5-Dihydro-
398 1Hpyrazolo[4,3-h] quinazoline Derivatives as Potent CDK2/Cyclin A Inhibitors Using 3D-QSAR and
399 Docking . *Int. J. Mol. Sci.* 2010, 11, 3705–3724.
- 400 [32]. Lan, P.; Chen W.N.; Chen W.M. Molecular modeling studies on imidazo[4,5-b]pyridine
401 derivatives as Aurora A kinase inhibitors using 3D-QSAR and docking approaches. *Eur. J. Med.*
402 *Chem.* 2011, 46, 77–94.
- 403 [33]. Lan, P.; Chen, W.N.; Xiao, G.K.; Sun, P.H.; Chen, W.M. 3D-QSAR and docking studies on
404 pyrazolo[4,3-h]quinazoline-3-carboxamides as cyclin-dependent kinase 2 (CDK2) inhibitors. *Bioorg.*
405 *Med. Chem. Lett.* 2010, 20, 6764–6772
- 406
- 407
- 408
- 409
- 410
- 411
- 412
- 413
- 414